

Aerosol mass loading over the marine environment of Arabian Sea during ICARB: Sea-salt and non-sea-salt components

SUSAN K GEORGE and PRABHA R NAIR*

Space Physics Laboratory, Vikram Sarabhai Space Centre, Thiruvananthapuram 695 022, India.

**e-mail: prabha_nair@vssc.gov.in*

Mass loading and chemical composition of atmospheric aerosols over the Arabian Sea during the pre-monsoon months of April and May have been studied as a part of the Integrated Campaign for Aerosols, gases and Radiation Budget (ICARB). These investigations show large spatial variabilities in total aerosol mass loading as well as that of individual chemical species. The mass loading is found to vary between 3.5 and 69.2 $\mu\text{g m}^{-3}$, with higher loadings near the eastern and northern parts of Arabian Sea, which decreases steadily to reach its minimum value in the mid Arabian Sea. The decrease in mass loading from the coast of India towards west is estimated to have a linear gradient of 1.53 $\mu\text{g m}^{-3}/^\circ$ longitude and an e^{-1} scale distance of ~ 2300 km. SO_4^{2-} , Cl^- and Na^+ are found to be the major ionic species present. Apart from these, other dominating water-soluble components of aerosols are NO_3^- (17%) and Ca^{2+} (6%). Over the marine environment of Arabian Sea, the non-sea-salt component dominates accounting to $\sim 76\%$ of the total aerosol mass. The spatial variations of the various ions are examined in the light of prevailing meteorological conditions and airmass back trajectories.

1. Introduction

The impact of aerosols on the weather and climate of the earth is one of the key research topics of recent times (Charlson *et al* 1992; Ramanathan *et al* 2001a; Kaufman *et al* 2002). Attempts are being made all over the globe to characterize the physical and chemical properties of aerosols to provide realistic inputs to various radiative forcing/climate prediction models. Critical assessment of the role of aerosols in radiative forcing is complicated by the fact that the physical and chemical properties of aerosols are highly variable in both time and space. For a complete characterization of the aerosol system over a region, information on their sources as well as the source strength is essential. While the topography decides the major natural aerosols originating over a region, the anthropogenic contribution

is decided by industries/human activities. Long-range transport of aerosols caused by the prevailing circulation systems make the situation even more complex. Knowledge on the chemical composition of aerosols is crucial in identifying the various sources and assessing the impact of long-range transport over a region (Prospero *et al* 1985; Carmichael *et al* 1997; Siefert *et al* 1999; Kulshrestha *et al* 2001; Rastogi and Sarin 2005; Yoon *et al* 2007).

Oceans are the single largest sources of natural aerosols. Through the mechanism of bubble bursting at the surface of the ocean, large amounts of sea-salt particles are injected into the atmosphere (Blanchard and Woodcock 1980; Fairall *et al* 1983; Exton *et al* 1985). Another important source contributing to the aerosol loading over oceans is the marine biogenic activity (Charlson *et al* 1987). Oxidation of dimethyl-sulphide (DMS) emitted by

Keywords. Atmospheric sciences; aerosols; climate; geochemistry; chemical composition of aerosols; sea-salt and non-sea-salt aerosols.

marine phytoplankton is a major source of non-sea-salt aerosols over remote oceanic areas (Savoie *et al* 1989; Kettle *et al* 1999). In addition, a considerable amount of anthropogenic and crustal aerosols also get transported to the marine environments (Hirose *et al* 1983; Savoie *et al* 1987, 2002; Garrett and Hobbs 1995; Arimoto *et al* 1996; Swap *et al* 1996; Kulshrestha *et al* 2001; Nair *et al* 2004a; Moorthy *et al* 2005a). In order to assess the effect of these transported anthropogenic/continental aerosols regular/periodic observations of the same is essential. *In situ* measurements of aerosols over the oceans are carried out mainly by campaign mode (ship-based) observations and/or from island stations. While island stations provide information on the seasonal variation of aerosol properties over the particular oceanic environment, ship-based campaign-mode measurements give information about their spatial variation over a vast oceanic region. Several cruises have been conducted during the last two decades as part of various investigative programmes like ACE (Aerosol Characterization Experiment), Aerosols99, PEM (Pacific Exploratory Mission), INDOEX (Indian Ocean Experiment), etc. for studying the spatial variations of aerosols over the marine environment (Arimoto *et al* 1996; Bates *et al* 1998; Huebert *et al* 1998; Satheesh *et al* 1998; Andreae *et al* 2000; Raes *et al* 2000; Ramanathan *et al* 2001b). A major cruise that focused on the aerosol characterization over the Indian Ocean (IO) and Arabian Sea (AS) is the INDOEX (Ramanathan *et al* 2001b) conducted in 1998–99. The pre-INDOEX cruises conducted since 1996 have also provided valuable information on the characteristics of aerosols and their effect on radiative forcing (Jayaraman *et al* 1998; Krishnamurti *et al* 1998). In addition to these, the cruises conducted as a part of the Arabian Sea Monsoon Experiment (ARMEX) also carried instruments to carry out studies on aerosols over the Arabian Sea (Moorthy *et al* 2005b; Rao *et al* 2005; Sunilkumar *et al* 2005).

This paper presents results from a dedicated field experiment – The Integrated Campaign for Aerosols, gases and Radiation Budget (ICARB), conceived under the Geosphere Biosphere Programme of Indian Space Research Organisation (ISRO-GBP) to assess the regional radiative impacts of aerosols and trace gases, and to quantify the effect of their long-range transport, involving the Indian mainland and adjoining oceans. As a part of ICARB, a one-month long cruise (Cruise SK 223B) was conducted over the Arabian Sea during the pre-monsoon months of April and May 2006, covering a major portion of the AS in the latitude sector of 9° to 22°N and a longitude sector of 58° to 76°E. This cruise covered a major portion of northern AS, which was left unexplored during

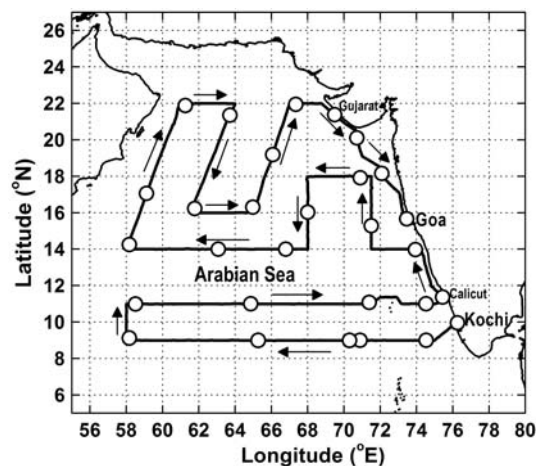


Figure 1. Cruise track of SK 223B over the Arabian Sea.

the previous cruises. The present study focused on the chemical characterization of aerosols over the AS, by carrying out *in situ* sampling at different regions over the cruise track and subsequent chemical analysis of the samples. The results on the spatial pattern of water-soluble components of atmospheric aerosols over the marine environment of AS are presented here. The observational results will contribute significantly to the database on aerosol characteristics over the AS region. Assimilating the results from the previous cruises, the seasonal changes in the chemical composition of aerosols over this tropical oceanic environment can be understood fairly well.

2. Cruise track of ICARB

The cruise SK 223B of ORV *Sagar Kanya* extended from 18 April 2006 to 11 May 2006. Figure 1 shows the cruise track. The arrowheads show the direction of movement of the ship and the open circles denote the mean positions from where aerosol samples were collected during the cruise. The ship started from Kochi (9.96°N, 76.3°E) on April 18 and then sailed westward along 9°N latitude to reach the farthest longitude, i.e., 58°E. Then it moved northward and then eastward along 11°N latitude to reach near Calicut coast on April 26. The subsequent track chosen was parallel to the coast up to ~14°N latitude, from where it had a longitudinal scan to reach 58°E longitude and then moving northward to reach the northernmost latitude (22°N). In this sector, the ship was sailing very close (150–200 km away) to the west Asian coast, after which it turned eastward. On reaching close to the Gujarat coast of India it sailed towards south to end the cruise at Goa (15.4°N, 73.8°E) on May 11. The cruise took 24 days to cover a latitude sector of 9° to 22°N and a longitude sector of

58° to 76°E of the AS and covered a distance of ~11430 km.

3. Instrumentation and data

3.1 Aerosol sampling

A single stage high volume sampler (Model GH2000 of Grasby Anderson, USA) was used for collecting total suspended particulates (TSP) over the AS. Quartz fibre filters of 4" diameter were used as the collection substrate. These substrates were pre-heated to above 100°C for about three hours to remove any volatile impurity and desiccated for 24 hours. Each substrate was then weighed using a microbalance (Model AT 20 of Mettler having a sensitivity of $\pm 2 \mu\text{g}$), carefully packed in self-sealing envelopes and taken to the ship for sampling. The sampler was calibrated before and after cruise to ascertain the flow rate. It was operated on the front deck of the ship to avoid the effect of any exhaust from the chimney. Samples were collected only when the ship was in motion. The wind direction was also monitored constantly during the sampling period to check the possibility of any contamination. The typical duration of sampling varied from 2 to 4 hours. After collection, each substrate was carefully sealed in envelopes, desiccated and brought back to the laboratory for further analysis. The sample-laden substrates were weighted again under the same laboratory conditions to estimate the mass of the samples collected in each of them. From the known flow rate and duration of sampling, the total aerosol mass loading (in $\mu\text{g m}^{-3}$) at the sampling location was estimated. About 30 aerosol samples were collected from discrete locations over the Arabian Sea during the cruise.

3.2 Chemical analysis

The samples collected during the cruise have been subjected to chemical analysis for identifying and quantifying its water-soluble components. The sample-laden substrates having an area of 20 cm² was cut out and extracted using de-ionized water (Milli-Q water with 18.2 M Ω resistivity) for analyzing the water-soluble fractions of various anions and cations. Ion Chromatography (IC) was employed for this purpose. Different ionic species identified using this technique are Cl⁻, NO₃⁻, SO₄²⁻, NH₄⁺, Na⁺, K⁺, Mg²⁺ and Ca²⁺. For the analysis of NH₄⁺, another identical piece of the substrate was extracted using de-ionized water without boiling, to avoid any possible loss of volatile ammonium species. An ion chromatograph DX-120 of Dionex equipped with

an anion exchange column IonPac AS14 and a cation exchange column IonPac CS12A was used for the separation and identification of the various species. A combination of 3.5 mM Na₂CO₃ and 1 mM NaHCO₃ was used as the eluent for anions and 20 mM solution of methane sulphonic acid (CH₃SO₃H) for cations. The eluent flow rate is fixed at 1 ml/min. The separated ions are detected using a conductivity detector.

4. Meteorological conditions during ICARB

Along with aerosol measurements, meteorological parameters viz., wind speed, wind direction, temperature, pressure, and relative humidity (RH) were also monitored during the entire cruise period using two Automatic Weather Stations (AWS) installed on both sides of the ship. In addition to this, hand-held meteorological instruments were also used to measure pressure, dry bulb temperature, wet bulb temperature, RH, wind speed and wind direction at an interval of one hour during the entire period. All these measurements are in good agreement within the respective uncertainty limits. The surface flow patterns obtained from NCEP/NCAR reanalysis (<http://www.cdc.noaa.gov>) have been used to ascertain the synoptic conditions. Air-mass back trajectories obtained using the Hybrid Single Particle Lagrangian Integrated Trajectory (HYSPLIT) model from NOAA ARL website (<http://www.arl.noaa.gov/ready.html>) have been used to investigate the origin of air-mass arriving at different locations over the study region to identify the major sources responsible for the observed aerosols.

Figure 2(a) and (b) shows the mean flow pattern (at 925 mb) over the AS for the months of April and May 2006. The arrow heads show the wind direction and the length of the arrow represents the mean wind speed. In April 2006, the ship was sailing over the southern parts of AS, between 9° and 14°N while in May 2006 it was sailing over its northern parts around 14–22°N. Note that April and May are transition months in which the synoptic wind changes from north easterlies to south westerlies. A region of anticyclonic flow was observed over the mid AS ~10–15°N in April 2006, where the wind speeds were in general low (1–3 ms⁻¹) and the cruise was mostly confined to this region. But in May, the ship generally experienced stronger winds (>6 ms⁻¹) originating mainly from southern oceanic regions. Figure 3(a) to (c) shows the day-to-day variation in daily mean wind speed (WS), relative humidity (RH), and air temperature (T) recorded from onboard

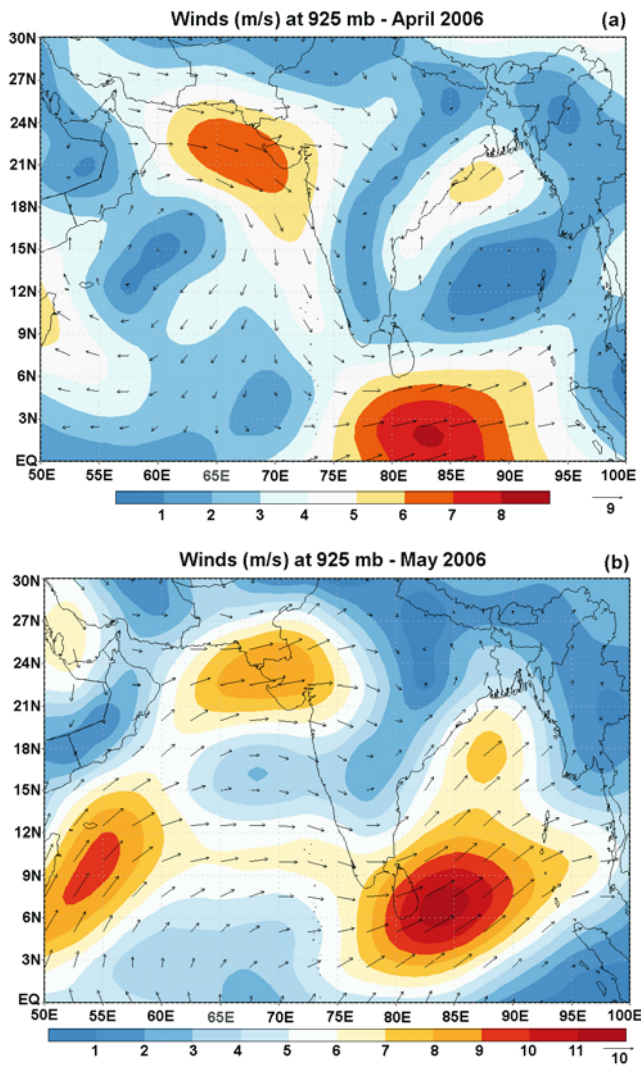


Figure 2. Synoptic wind patterns at 925 mb level over Arabian Sea for (a) April 2006 and (b) May 2006.

measurements. During 18 to 23 April 2006, while the ship was sailing over the southern parts of AS, wind speeds were $< 6 \text{ ms}^{-1}$ and as the ship moved towards north, the wind speed increased reaching as high as $15\text{--}16 \text{ ms}^{-1}$ (with a daily mean of around 10 ms^{-1}) on 26 April, 4 May and 8 May 2006. The RH was found to be almost steady around 70–75% during April, which increased to $\sim 90\%$ by 8–9 May 2006. The air temperature was around 28–30°C during the cruise period which was devoid of any rain event.

5. Results and discussion

5.1 Spatial variation of aerosol mass loading over the Arabian Sea

The mean aerosol mass concentration (M_L) was $\sim 35 \pm 17 \mu\text{g m}^{-3}$ over the AS. The highest value of

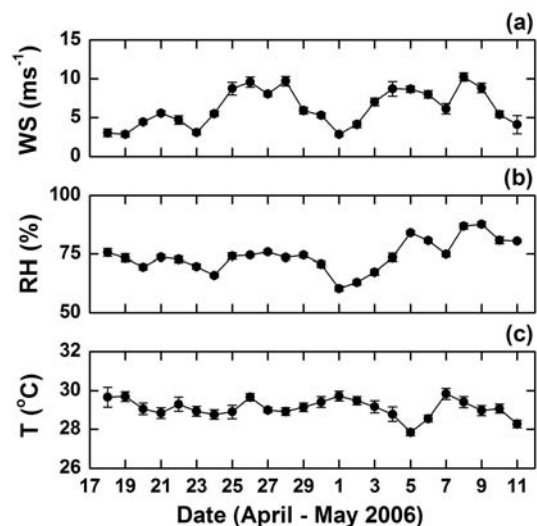


Figure 3. Day-to-day variation of meteorological parameters (a) wind speed, (b) relative humidity and (c) air temperature during the cruise period.

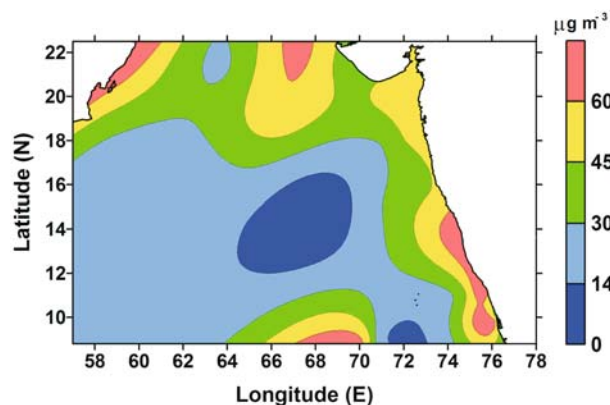


Figure 4. Spatial variation of total aerosol mass concentration over the Arabian Sea.

$69.2 \mu\text{g m}^{-3}$ was observed around 11.4°N , 75.4°E while the extremely low value of $3.5 \mu\text{g m}^{-3}$ was encountered around 14°N , 66.8°E . Figure 4 illustrates the spatial variation in M_L observed over the AS during the cruise period. It shows a prominent region of low M_L over the mid AS. Close to the western coast of Indian peninsula and over the northern AS regions, M_L is large. It decreases gradually from the coastal regions towards west. Another region of high M_L is observable in the southern part of AS around 14°N and 67°E . The region of low M_L lies in the region of anticyclonic flow (figure 2a). The wind vectors around this region show weak divergence. This is also the region of low wind speed. The high near the coastal regions can be attributed to continental influence. The high M_L over the northern AS could most probably be attributed to *in situ* production of sea

Table 1. A comparison between the mean mass loading (M_L) observed during various cruises over the Arabian Sea.

| Campaign | Period of study | Oceanic region | Mean M_L ($\mu\text{g m}^{-3}$) | Reference |
|------------|------------------------------|-----------------|--|---------------------------|
| INDOEX-FFP | February–March 1998 (winter) | 8–15°N, 56–77°E | ~38 | Nair <i>et al</i> (2004a) |
| INDOEX-IFP | January–March 1999 (winter) | 8–17°N, 56–77°E | ~35 | Nair <i>et al</i> (2004a) |
| ARMEX-IIA | April–May 2005 (pre-monsoon) | 8.3°N, 72.6°E | ~24 | Our own observations |
| ICARB | April–May 2006 (pre-monsoon) | 9–22°N, 58–75°E | ~29.6 | Present study |

spray aerosols produced by surface wind and/or due to the intrusion from nearby landmasses which can be ascertained only through chemical characterization and air trajectories which are addressed in later sections.

Similar measurements on aerosol mass loading carried out in different years as part of INDOEX and ARMEX are presented in table 1, along with those obtained during the present investigation, averaged over a common region (above 8°N and away from coastal regions) for a direct comparison. This table shows that the mass loading is large during winter compared to that during the summer/pre-monsoon period. This can mainly be attributed to synoptic circulation. While during winter, the synoptic flow near surface is mainly from west Asia and peninsular India, that during summer/pre-monsoon period is mostly centred over the Arabian Sea region (resulting only in local production).

5.2 Latitudinal and longitudinal variations in mass loading

The longitudinal/latitudinal variations in aerosol mass loading were estimated by grouping them according to the different regions from where the samples had been collected. To examine the latitudinal variation, samples collected between 9°N and 11°N were grouped to represent the Southern Arabian Sea (SAS), those between 14°N and 17°N were grouped to represent the Mid Arabian Sea (MAS) and those in the latitude sector 18–22°N represent the Northern Arabian Sea (NAS). But it is evident from figure 4 that irrespective of the latitudes, the mass loading is large near the coastal regions of peninsular India. Because of this feature, coastal samples were excluded before averaging them along different latitude bins. These averages are plotted in figure 5(a). Vertical bars indicate the standard error. As can be seen from this figure, the mass loading is large over the NAS (2.5 times larger than that over MAS). The mean

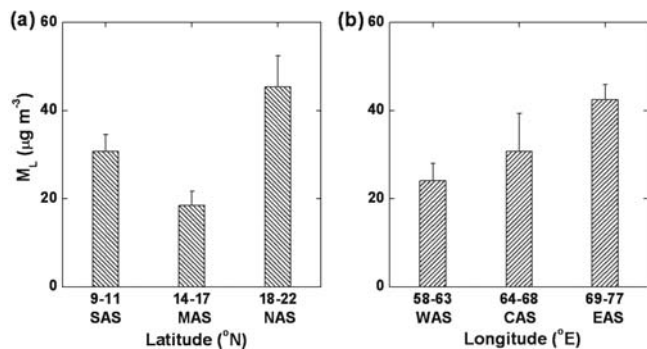


Figure 5. Variation of total aerosol mass concentration along different (a) latitude sectors and (b) longitude sectors.

M_L over SAS is also ~1.7 times larger than that over MAS.

Since the aerosol properties are region-specific, the longitudinal gradients were first examined by grouping the data corresponding to the different latitudinal sectors mentioned above (NAS, MAS and SAS). Figure 6(a) to (c) shows the longitudinal variation of aerosol mass loading in these three distinct regions. It was observed that in SAS and MAS, M_L has an increasing trend eastward whereas in NAS no longitudinal dependence of M_L was observed. The longitudinal gradients in SAS and MAS were obtained by performing the linear regression analysis of the corresponding data (figure 6a and b) and found to be $1.4 \mu\text{g m}^{-3}/^\circ$ in SAS and $2.23 \mu\text{g m}^{-3}/^\circ$ in MAS. In order to have an overall understanding of the longitudinal variation of mass loading in the study region (as in the case of latitudinal variation discussed above), the samples were again grouped and averaged according to their longitude irrespective of latitude. For this, the samples collected in the longitude sector 58–63°E have been grouped together to represent the Western Arabian Sea (WAS), those in the longitude sector 64–68°E to represent the Central Arabian Sea (CAS) and those collected between 69°E and 77°E to represent the Eastern Arabian

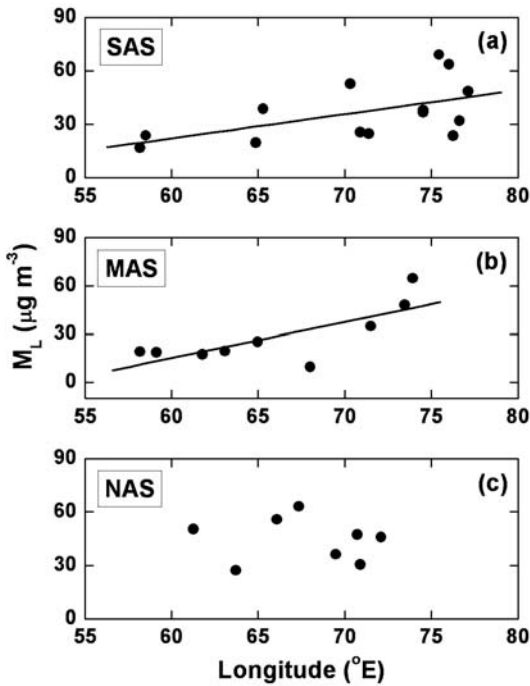


Figure 6. Longitudinal variation in mass loading in (a) southern, (b) mid and (c) northern Arabian Sea.

Sea (EAS). The longitudinal variation in mean mass loading is presented in figure 5(b) with bars denoting the standard error. The mean mass loading increases with increase in longitude. The linear gradient is $1.53 \mu\text{g m}^{-3}/^\circ$ longitude as obtained by the linear regression analysis. The exponential gradient of M_L across the longitude has also been examined by using logarithmic regression, which yielded a scale distance (distance at which M_L decreases by a factor of e^{-1}) of ~ 2300 km towards west. It would be of worth in this context to note that a similar east-west gradient has been reported for aerosol mass loading (decrease in M_L from east to west) from measurements carried out during the INDOEX (Nair *et al* 2004a) which was marginally less than that obtained from the present study. Also during INDOEX, the scale distance estimated over the northern hemispheric oceanic regions was ~ 6880 km (Nair *et al* 2004a), which is substantially higher than that obtained during the present study. This indicates that the gradient in M_L is relatively large during pre-monsoon months compared to that during the winter, probably due to higher wind speeds.

Over the EAS and NAS, the mass loadings are comparable and may be attributed to the aerosols advected from the nearby continent under the influence of prevailing synoptic circulation. A similar high in M_L along the west coast of India was observed during INDOEX period also, which is attributed to continental impact (Ball *et al* 2003;

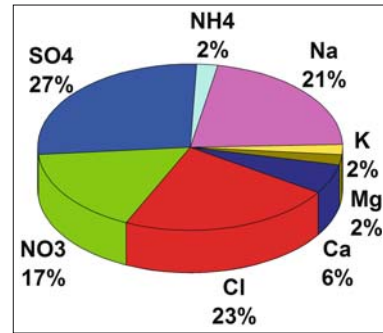
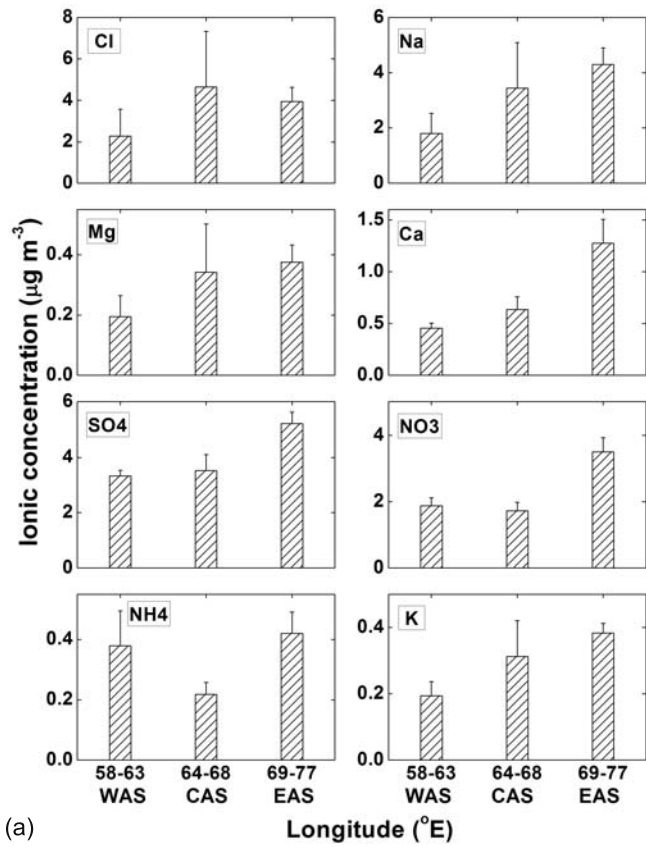


Figure 7. Mean percentage contribution of water-soluble components.

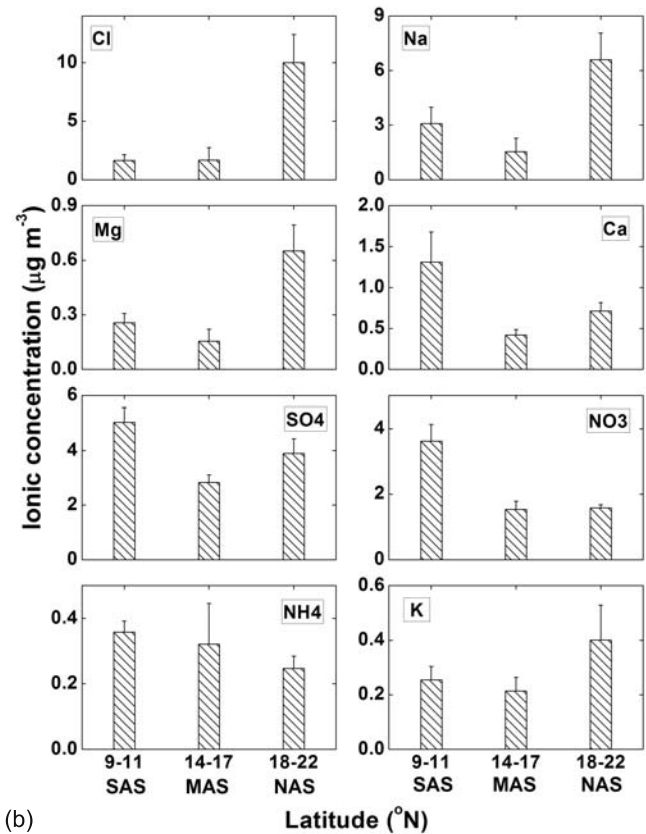
Nair *et al* 2004a, b). Close to the Indian coast, M_L values reported during the First Field Phase (FFP) of INDOEX lie in the range $21\text{--}53 \mu\text{g m}^{-3}$ (Nair *et al* 2004a), which is comparable to those observed in the present study ($23\text{--}69 \mu\text{g m}^{-3}$). While a region of high M_L was observed over the mid AS during INDOEX period (Nair *et al* 2004a), a low M_L is observed in the present study. As stated above, this could mainly be attributed to the difference in synoptic circulation.

5.3 Chemical composition of aerosols over the cruise region

The chemical analysis of the water-soluble fractions of aerosol samples collected during the cruise revealed SO_4^{2-} and Cl^- to be the major anions. The percentage contributions of these ions were found to be about 27% and 23% respectively. Among the cations, Na^+ (which is the major component of sea water) was found to be the most dominant species with a mean percentage contribution of $\sim 21\%$. While Ca^{2+} , which has oceanic as well as crustal sources, contributed $\sim 6\%$ to the total water soluble mass, the percentage contribution of other cations, viz., NH_4^+ , Mg^{2+} and K^+ added up to $\sim 6\%$. The pie diagram in figure 7 shows the mean percentage contribution of various water-soluble ions to aerosol mass. Different ionic components revealed from the analysis were grouped in different longitude/latitude sectors, as in the case of total mass, and averaged, a plot of which is presented in figure 8(a) and (b). Figure 8(a) shows that the highest concentration of all ions (except Cl^-) are encountered over the EAS, i.e., close to the coastal regions of peninsular India, and the lowest values are observed over the WAS. This shows that the longitudinal pattern of most of the ions is similar to that of the total aerosol mass. But in the case of Cl^- , the concentration peaks over the CAS with low values over the WAS region. In the case of NH_4^+ , the concentration over WAS was found to be



(a)



(b)

Figure 8. (a) Longitudinal variation in the ionic concentration of various species and (b) latitudinal variation in the ionic concentration of various species.

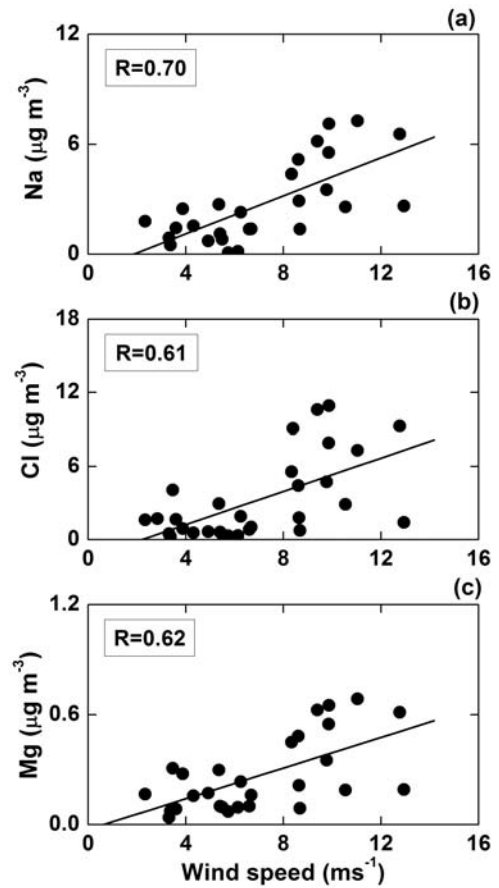


Figure 9. Wind dependence of (a) Na, (b) Cl and (c) Mg.

comparable to that over EAS and lower values were measured over CAS. The major sources of NH_4^+ being agricultural activities, domestic animals, etc. (Zhao and Wang 1994), which are located over the land, the concentration of this species may decrease towards the open ocean. The latitudinal variation of the concentration of some of the ions, like Na^+ , K^+ and Mg^{2+} , presented in figure 8(b), shows a similar pattern to that of total aerosol mass (with low values over MAS). While the concentration of Cl^- is found to be largest over NAS, that over MAS and SAS are comparable. Other ions, viz., SO_4^{2-} , NO_3^- , NH_4^+ and Ca^{2+} show higher values over the SAS compared to those over NAS. While the lowest concentration of NH_4^+ is observed over NAS, that of the other three ions are observed over MAS.

From the latitudinal patterns it is clear that the concentration of major ions of sea-salt origin, viz., Na^+ , Cl^- and Mg^{2+} shows a prominent peak over NAS. As seen in section 4, the wind speed is large during May (figures 2b and 3a) when the ship was sailing along the northern AS. As can be seen from various other investigations, the sea-salt production over the ocean strongly depends on wind speed (Monahan *et al* 1983; Exton *et al* 1985).

To examine this feature in terms of chemical composition, the wind speed dependence of the concentration of Na^+ , Cl^- , and Mg^{2+} are examined through linear regression analysis. This analysis showed that the concentrations of these ions are well correlated with wind speed with a correlation coefficient of 0.70, 0.61 and 0.62 respectively (figure 9a to c). Hence, the observed spatial distribution of these ions over the AS could be attributed to wind. The concentrations of other ions, like SO_4^{2-} , NO_3^- , NH_4^+ , and Ca^{2+} , which are mainly of anthropogenic/continental origin, are found to be highest over the EAS and SAS. The increased concentration of these ions over the EAS can be attributed to their proximity to the continent. On the other hand, the high over SAS can be explained partly on the basis of airflow pattern and air mass back trajectories discussed in section 5.5 and shown in figure 12(d). When the ship was sailing across SAS region (during the month of April) it encountered winds mainly from north/north-west traversing the north western landmass and coastal regions of India (figure 2a). The observed increase in concentration of anthropogenic/continental species might have been caused by advection.

5.4 Sea-salt and non-sea-salt aerosols

Aerosols over the oceanic regions are expected to be dominated by particles originating from sea-spray notwithstanding the intrusion of continental/ anthropogenic aerosols through long-range transport. Major sea-salt associated ions are identified using Na^+ as the reference element. The linear regression analysis of Na^+ against Cl^- and Mg^{2+} yielded high positive correlation with coefficients of 0.89 and 0.99 respectively, confirming that they are of the same origin (from sea-spray). From the measured concentrations of Na^+ and Cl^- , the mass concentration of sea-salt aerosols can be estimated using the empirical relation (Holland 1978)

$$M_{\text{ss}} = M_{\text{Cl}} + 1.47 \times M_{\text{Na}}, \quad (1)$$

where M_{ss} , M_{Cl} , and M_{Na} represent the mass of sea-salt, Cl and Na respectively. The coefficient, 1.47, is the sea water ratio of $(\text{Na}^+ + \text{K}^+ + \text{Mg}^{2+} + \text{Ca}^{2+} + \text{SO}_4^{2-} + \text{HCO}_3^-)/\text{Na}^+$. This approach eliminates the inclusion of non-sea-salt K^+ , Mg^{2+} , Ca^{2+} , SO_4^{2-} and HCO_3^- in the sea-salt mass and allows for the loss of Cl^- through depletion process. The sea-salt concentration thus estimated over the AS is found to vary from 0.4 to $35.6 \mu\text{g m}^{-3}$ with an average concentration of $8.8 \mu\text{g m}^{-3}$. This mean sea-salt concentration accounts for $\sim 46\%$ of the

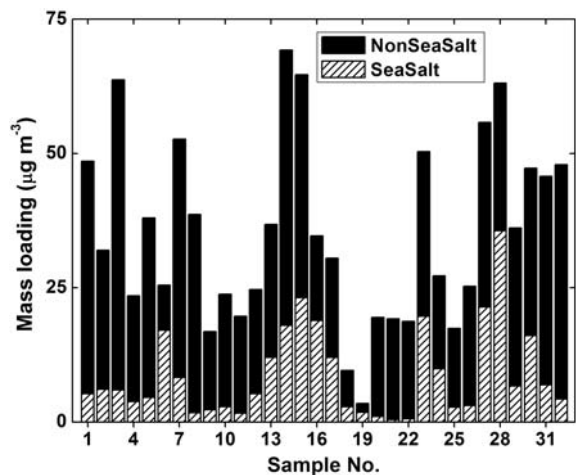


Figure 10. Sample-to-sample variation in the mass loading of sea-salt and non-sea-salt components.

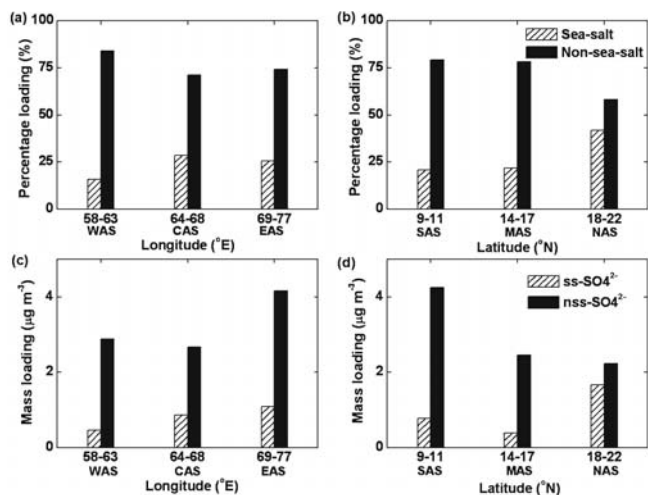


Figure 11. Percentage contribution of sea-salt and non-sea-salt components of aerosol mass loading at different longitude and latitude sectors (a and b). Mass loading of ss and nss- SO_4^{2-} in total SO_4^{2-} at different longitude and latitude sectors (c and d).

water soluble mass and $\sim 24\%$ of total mass loading of aerosols collected during the cruise period. The non-sea-salt mass (M_{nss}) can be estimated from M_L and M_{ss} as

$$M_{\text{nss}} = M_L - M_{\text{ss}}. \quad (2)$$

The mean M_{nss} is found to be $\sim 27 \mu\text{g m}^{-3}$, which amounts to $\sim 76\%$ of the total aerosol mass loading over the AS. Figure 10 shows the sample-to-sample variation in sea-salt and non-sea-salt mass during the cruise period. Note that the analysis of aerosol samples collected during the INDOEX cruise (Nair *et al* 2004b) indicated that mass

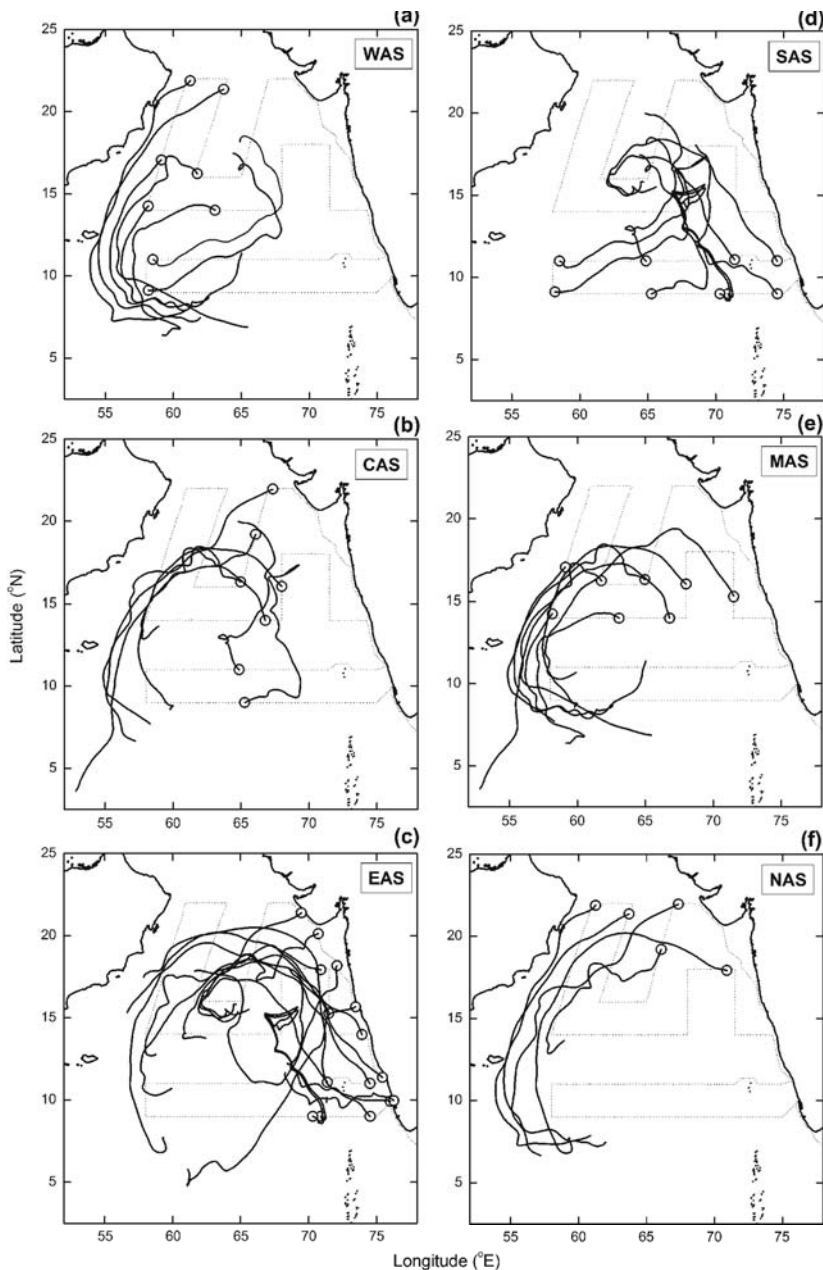


Figure 12. Seven-day back trajectories reaching (a) WAS, (b) CAS, (c) EAS, (d) SAS, (e) MAS and (f) NAS.

concentration of sea-salt aerosols are in the range $1\text{--}15\ \mu\text{g m}^{-3}$. A comparison of the estimated sea-salt and non-sea-salt components in aerosol mass during the present cruise with those during the INDOEX period indicates an increased sea-salt production during the present study period, which is quite expected because of prevailing high wind speeds. The percentage contributions of sea-salt and non-sea-salt components to total aerosol mass were grouped in different longitude and latitude sectors as in the previous cases to examine their spatial variations. Longitudinally, the sea-salt contribution is slightly larger over the EAS and CAS regions and low over the WAS region (figure 11a),

while the opposite is true for non-sea-salt component. Along the latitude, the sea-salt component steadily increases with the increase in latitude while the non-sea-salt component is largest in the SAS and MAS regions and low over the NAS region (figure 11b).

The SO_4^{2-} component in aerosols is considered to be a tracer for anthropogenic influence. However, over the oceans and coastal sites SO_4^{2-} has both sea-salt and non-sea-salt components (Prospero 2002). The sea salt component is estimated using Na as the reference element based on the empirical relation (Duce *et al* 1983),

$$M_{\text{ss}}\text{SO}_4 = 0.25 \times M_{\text{Na}}, \quad (3)$$

where $M_{\text{ss}}\text{SO}_4$ is the mass of sea-salt component of SO_4^{2-} , M_{Na} is the mass of Na and the coefficient 0.25 represent the mass ratio of SO_4^{2-} to Na in sea water (Berg and Winchester 1978). Subtracting this component from the total measured SO_4^{2-} , the non-sea-salt SO_4^{2-} is also estimated for each sample. The mass loading of nss- SO_4^{2-} is found to vary from 1.38 to $7.15 \mu\text{g m}^{-3}$. It would be worth mentioning in this context that the concentration of nss- SO_4^{2-} reported for regions north of ITCZ during INDOEX lie in the range $2.2\text{--}18.31 \mu\text{g m}^{-3}$ (Kulshrestha *et al* 2001), which is higher than the values obtained during the present study. The mean concentration of nss- SO_4^{2-} measured north of ITCZ during the pre-INDOEX cruise typically ranged from $1\text{--}4 \mu\text{g m}^{-3}$ with values as high as $9 \mu\text{g m}^{-3}$ (Krishnamurti *et al* 1998). This indicates that the advection of continental aerosols over to the oceanic regions is less during pre-monsoon compared to the winter season during which both the above-mentioned cruises were conducted. Figure 11(c) and (d) shows the mean concentration of ss and nss- SO_4^{2-} for the same sectors as in figure 11(a) and (b). Figure 11(c) and (d) show the dominance of nss- SO_4^{2-} over the AS region with highest concentrations over EAS and SAS. While the high concentration of nss- SO_4^{2-} over EAS can be due to its proximity to coastal regions, that over SAS can be attributed to airflow pattern favouring the advection of continental aerosols from the north as discussed in section 5.3.

5.5 Back trajectory analysis

The airmass back trajectories are obtained by running the HYSPLIT model from NOAA ARL website (Draxler and Rolph 2003; Rolph 2003). Considering the low residence time of aerosols near the surface, a seven-day back trajectory of airmass reaching the mean position of sampling has been examined. Those trajectories ending at 100 m above the sea-surface (which is well within the marine boundary layer over the AS during the cruise period) were considered for the present analysis. These trajectories were further grouped according to the longitudinal/latitudinal sectors as detailed in section 5.2 and are presented in figure 12(a–f). A close examination of these trajectories shows that all the back trajectories have their origin over the oceanic region. But, the back trajectories in the SAS (figure 12d) have their origin in the northern AS whereas in all other regions they originate from the southern open oceanic environments. The high loading

of continental aerosols over SAS may be partly attributed to this. However, it can be inferred that the airmass prevailing over the AS region during the study period is of marine origin and the measurements are pertaining to marine boundary layer aerosols.

6. Conclusions

Spatial variations in total aerosol mass loading as well as its water soluble components are studied over the Arabian Sea during the pre-monsoon cruise of ICARB. An important feature revealed from this study is the high mass concentration of aerosols over the northern parts of the Arabian Sea and along the west coast of India. Chemical analysis revealed that SO_4^{2-} , Cl^- and Na^+ are the major ions contained in these samples. The percentage contribution of sea-salt to total aerosol mass estimated from the concentration of Na^+ and Cl^- is $\sim 26\%$ over the cruise region. The latitudinal and longitudinal variation of total aerosol mass loading and its chemical constituents are examined in detail. The total mass loading is found to decrease towards west from the west coast of peninsular India with a gradient of $1.53 \mu\text{g m}^{-3}/^\circ$ longitude and a scale distance of ~ 2300 km. The mass concentration of Na^+ , Cl^- and Mg^{2+} , which are mostly of sea-spray origin, shows a significant dependence on wind speed. The concentrations of these ions steadily increase with increase in wind speed.

Acknowledgements

The NCEP/NCAR reanalysis is obtained from NOAA-CIRES Climate Diagnostics Center, Boulder, Colorado from their website <http://www.cdc.noaa.gov>. The authors gratefully acknowledge the NOAA Air Resources Laboratory (ARL) for the provision of the HYSPLIT transport and dispersion model and/or READY website (<http://www.arl.noaa.gov/ready.html>) used in this publication. The authors are grateful to Dr. K Parameswaran for going through the manuscript and for his valuable suggestions.

References

- Andreae M O, Elbert W, Gabriel R, Johnson D W, Osborne S and Wood R 2000 Soluble ion chemistry of the atmospheric aerosol and SO_2 concentrations over the eastern North Atlantic during ACE-2; *Tellus* **52B** 1066–1087.
- Arimoto R, Duce R A, Savoie D L, Prospero J M, Talbot R, Cullen J D, Tomza U, Lewis N F and Ray B J 1996 Relationship among aerosol constituents from Asia and the North Pacific during PEM-West A; *J. Geophys. Res.* **101(D1)** 2011–2023.

- Ball W P, Dickerson R R, Doddridge B G, Stehr J W, Miller T L, Savoie D L and Carsey T P 2003 Bulk and size-segregated aerosol composition observed during INDOEX 1999: Overview of meteorology and continental impacts; *J. Geophys. Res.* **108**(D10) 8001 doi:10.1029/2002JD002467.
- Bates T S, Huebert B J, Gras J L, Griffiths F B and Durkee P A 1998 International Global Atmospheric Chemistry (IGAC) Project's First Aerosol Characterization Experiment (ACE 1): Overview; *J. Geophys. Res.* **103** 16,297–16,318.
- Berg W W Jr and Winchester J W 1978 Aerosol chemistry of marine atmosphere. In: *Chemical Oceanography* (eds) J P Riley and R Chester (London: Academic Press) **7** 173–231.
- Blanchard D C and Woodcock A H 1980 The production, concentration, and vertical distribution of the sea-salt aerosol; *Ann. N. Y. Acad. Sci.* **338** 330–347.
- Carmichael G R, Hong M S, Ueda H, Chen L L, Murano K, Park J K, Lee H, Kim Y, Kang C and Shim S 1997 Aerosol composition at Cheju Island, Korea; *J. Geophys. Res.* **102** 6047–6061.
- Charlson R J, Lovelock J E, Andreae M O and Warren S G 1987 Oceanic phytoplankton, atmospheric sulfur, cloud albedo and climate; *Nature* **326** 655–661.
- Charlson R J, Schwartz S E, Hales J M, Cess R D, Coakley Jr. J A, Hansen J E and Hofmann D J 1992 Climate forcing by anthropogenic aerosols; *Science* **255** 423–430.
- Draxler R R and Rolph G D 2003 HYSPLIT (HYbrid Single-Particle Lagrangian Integrated Trajectory) Model access via NOAA ARL READY Website (<http://www.arl.noaa.gov/ready/hysplit4.html>). NOAA Air Resources Laboratory, Silver Spring, MD.
- Duce R A, Arimoto R, Ray B J, Unni C K and Harder P J 1983 Atmospheric trace elements at Enewetak Atoll 1. concentrations, sources and temporal variability; *J. Geophys. Res.* **88** 5321–5342.
- Exton H J, Latham J, Park P M, Perry S J, Smith M H and Allan R R 1985 The production and dispersal of marine aerosol; *Q. J. R. Meteorol. Soc.* **111** 817–837.
- Fairall C W, Davidson K L and Schacher G E 1983 An analysis of the surface production of sea-salt aerosols; *Tellus* **35B** 31–39.
- Garret T J and Hobbs P V 1995 Long range transport of continental aerosols over the Atlantic Ocean and their effect on cloud structures; *J. Atmos. Sci.* **52** 2977–2984.
- Hirose K, Dokiya Y and Sugimura Y 1983 Effect of the continental dust over the North Pacific Ocean: time variation of chemical components in maritime aerosol particles in spring season; *J. Meteorol. Soc. Japan* **61** 670–677.
- Holland H D 1978 *The Chemistry of the Atmosphere and Oceans* (New York: Wiley).
- Huebert B J, Howell S G, Zhuang L, Heath J A, Litchy M R, Wylie D J, Kreidler-Moss J I, Coppicus S and Pfeiffer J E 1998 Filter and impactor measurements of anions and cations during the First Aerosol Characterization Experiment (ACE 1); *J. Geophys. Res.* **103** 16,493–16,509.
- Jayaraman A, Lubin D, Ramachandran S, Ramanathan V, Woodbridge E, Collins W D and Zalpuri K S 1998 Direct observations of aerosol radiative forcing over the tropical Indian Ocean during the January–February 1996 pre-INDOEX cruise; *J. Geophys. Res.* **103**(D12) 13,827–13,836.
- Kaufman Y J, Tanre D and Boucher O 2002 A satellite view of aerosols in the climate system; *Nature* **419** 215–223.
- Kettle A J *et al* 1999 A global database of sea surface dimethylsulfide (DMS) measurements and a procedure to predict sea surface DMS as a function of latitude, longitude and month; *Global Biogeochem. Cyc.* **13** 399–444.
- Krishnamurti T N, Jha B, Prospero J M, Jayaraman A and Ramanathan V 1998 Aerosol and pollutant transport and their impact on radiative forcing over the tropical Indian Ocean during the January–February 1996 pre-INDOEX cruise; *Tellus* **50B** 521–542.
- Kulshrestha U C, Jain M, Sekar R, Vairamani M, Sarkar A K and Parashar D C 2001 Chemical characteristics and source apportionment of aerosols over Indian Ocean during INDOEX-1999; *Curr. Sci.* **80** 180–185.
- Monahan E C, Fairall C W, Davidson K L and Boyle P J 1983 Observed inter relation between 10 m winds, ocean whitecaps and marine aerosols; *Q. J. R. Meteorol. Soc.* **109** 379–392.
- Moorthy K K, Satheesh S K, Babu S S and Saha A 2005a Large latitudinal gradients and temporal heterogeneity in aerosol black carbon and its mass mixing ratio over southern and northern oceans observed during a trans-continental cruise experiment; *Geophys. Res. Lett.* **32** L14818 doi:10.1029/2005GL023267.
- Moorthy K K, Babu S S and Satheesh S K 2005b Aerosol characteristics and radiative impacts over the Arabian Sea during the intermonsoon season: Results from ARMEX field campaign; *J. Atmos. Sci.* **62** 192–206.
- Nair P R, Parameswaran K, Sunilkumar S V and Rajan R 2004a Continental influence on the spatial distribution of particulate loading over the Indian Ocean during winter season; *J. Atmos. Solar Terr. Phys.* **66** 27–38.
- Nair P R, Parameswaran K, Sunilkumar S V, Abraham A and Jacob S 2004b Chemical composition of atmospheric aerosols over the Indian Ocean: Impact of continental advection; *Adv. Space Res.* **34** 828–832.
- Prospero J M 2002 The Chemical and Physical Properties of Marine Aerosols: An Introduction; In: *Chemistry of Marine Water and Sediments* (eds) A Gianguzza, E Pellizzetti and S Sammarano (Berlin Heidelberg: Springer-Verlag) pp 35–82.
- Prospero J M, Savoie D, Nees R T, Duce R A and Merrill J 1985 Particulate sulphate and nitrate in the boundary layer over the North Pacific Ocean; *J. Geophys. Res.* **90** 10,586–10,596.
- Raes F, Bates T, McGovern F and Van Liedekerke M 2000 The 2nd Aerosol Characterization Experiment (ACE-2): general overview and main results; *Tellus* **52B** 111–125.
- Ramanathan V, Crutzen P J, Kiehl J T and Rosenfeld D 2001a Aerosols, climate, and the hydrological cycle; *Science* **294** 2119–2124.
- Ramanathan V, Crutzen P J, Lelieveld J *et al* 2001b The Indian Ocean Experiment: An integrated analysis of the climate forcing and effects of the Great Indo-Asian Haze; *J. Geophys. Res.* **106**(D22) 28,371–28,398.
- Rao P S P, Praveen P S, Chate D M, Ali K, Safai P D and Momin G A 2005 Physical and chemical characteristics of aerosols over Arabian Sea during ARMEX 2002-03; *Mausam* **56**(1) 293–300.
- Rastogi N and Sarin M M 2005 Long-term characterization of ionic species in aerosols from urban and high-altitude sites in western India: Role of mineral dust and anthropogenic sources; *Atmos. Environ.* **39** 5541–5554.
- Rolph G D 2003 Real-time Environmental Applications and Display sYstem (READY) Website (<http://www.arl.noaa.gov/ready/hysplit4.html>). NOAA Air Resources Laboratory, Silver Spring, MD.
- Satheesh S K, Moorthy K K and Murthy B V K 1998 Spatial gradients in aerosol characteristics over the Arabian Sea and Indian Ocean; *J. Geophys. Res.* **103** 26,183–26,192.

- Savoie D L, Prospero J M and Nees R T 1987 Nitrate, non-sea-salt sulfate, and mineral aerosol over the northwestern Indian Ocean; *J. Geophys. Res.* **92(D1)** 933–942.
- Savoie D L, Prospero J M, Merrill J T and Uematsu M 1989 Nitrate in the atmospheric boundary layer of the tropical South Pacific: Implications regarding sources and transport; *J. Atmos. Chem.* **8** 391–415.
- Savoie D L, Arimoto R, Keene W C, Prospero J M, Duce R A and Galloway J N 2002 Marine biogenic and anthropogenic contributions to non-sea-salt sulfate in the marine boundary layer over the North Atlantic Ocean; *J. Geophys. Res.* **107(D18)** 4356 doi:10.1029/2001JD000970.
- Siefert R L, Johansen A M and Hoffmann M R 1999 Chemical characterization of ambient aerosol collected during the southwest monsoon and intermonsoon seasons over the Arabian Sea: Labile-Fe (II) and other trace metals; *J. Geophys. Res.* **104** 3511–3526.
- Sunilkumar S V, Nair P R and Parameswaran K 2005 Aerosol size distribution over the Arabian Sea during ARMEX-II; *Mausam* **56(1)** 321–326.
- Swap R, Garstang M, Macko S A, Tyson P D, Maenhaut W, Antaxo P, Kallberg P and Talbot R 1996 The Long range transport of southern African Aerosols to the tropical South Atlantic; *J. Geophys. Res.* **101** 23,777–23,791.
- Yoon Y J *et al* 2007 Seasonal characteristics of the physicochemical properties of North Atlantic marine atmospheric aerosols; *J. Geophys. Res.* **112** D04206 doi:10.1029/2005JD007044.
- Zhao D W and Wang A P 1994 Estimation of anthropogenic ammonia emissions in Asia; *Atmos. Environ.* **28(4)** 689–694.

MS received 15 August 2007; revised 29 October 2007; accepted 29 November 2007